



## ANALYSIS OF DYNAMICAL PROPERTIES OF A 700 kW TURBINE ROTOR DESIGNED TO OPERATE IN AN ORC INSTALLATION

Lukasz BREŃKACZ, Grzegorz ŻYWICA, Małgorzata BOGULICZ

The Szewalski Institute of Fluid-Flow Machinery, Polish Academy of Sciences  
Centre of Mechanics of Machines, Department of Turbine Dynamics and Diagnostics  
Gen. J. Fiszer 14 St. 80-231 Gdańsk, Poland, [lbrenkacz@imp.gda.pl](mailto:lbrenkacz@imp.gda.pl)

### Summary

The article presents the results of structural and dynamic analyses carried out for an axial-flow turbine with a capacity of 700 kW. The turbine is specifically designed for operation in an ORC (Organic Rankine Cycle) installation. The turbine rotor was supported by the following hydrodynamic bearings: two radial bearings and one bidirectional axial bearing. During numerical computation, both forces affecting the blade system and the rotor's torsional moments affecting the shaft were taken into account. Static, modal and forced vibration analysis of the turbine rotor was presented. The article also discusses the process of bearing selection and their geometry optimization to keep the rotor vibration level as low as possible. The computations of radial hydrodynamic bearings were carried out for various bearing clearance shapes. Madyn 2000 software and the in-house developed computer programs that are included in the MESWIR system were used during computer modeling.

Keywords: ORC turbine, rotor dynamics, hydrodynamic bearings.

### ANALIZA WŁAŚCIWOŚCI DYNAMICZNYCH WIRNIKA TURBINY 700 kW ZAPROJEKTOWANEJ DO WYKORZYSTANIA W INSTALACJI ORC

#### Streszczenie

W artykule przedstawiono wyniki analizy wytrzymałościowej i dynamicznej turbiny osiowej o mocy 700 kW. Turbina zaprojektowana została do pracy w obiegu ORC (Organic Rankine Cycle). Wirnik turbiny łożyskowany był za pomocą dwóch poprzecznych łożysk hydrodynamicznych oraz dwukierunkowego hydrodynamicznego łożyska osiowego. W obliczeniach numerycznych uwzględniono siły działające na układ łopatkowy oraz momenty skrętne działające na wirnik. Przedstawione zostały analiza statyczna, analiza modalna oraz analiza drgań wymuszonych. Zaprezentowany został proces doboru łożysk i optymalizacja ich geometrii pod kątem minimalizacji drgań wirnika. Wykonane zostały obliczenia poprzecznych łożysk hydrodynamicznych dla różnych kształtów szczeliny smarnej. Podczas pracy użyty został program Madyn 2000 oraz programy ze środowiska MESWIR opracowane w IMP PAN w Gdańsku.

Słowa kluczowe: turbina ORC, dynamika wirnika, łożyska hydrodynamiczne.

## 1. INTRODUCTION

The article presents the results of kinetostatic and dynamic analyses of a newly designed turbine with a capacity of 700 kW operating in an ORC installation. This is a prototypical turbine and dynamic properties of this kind of turbines have not been widely described in literature. In the frame of this work modern tools were used to perform the entire design process ensuring good dynamic properties. The example of an ORC system is described in the paper [1]. The diagram of the ORC system is presented in Fig. 1. The main components of this system are the following: turbine marked with T and three heat exchangers (that is, evaporator, regenerator and condenser) marked with E, R and C, respectively. The calculation examples for elements of this type are shown in the paper [2].

The boiler, marked with B, was used for heating working medium. A pump (P) directly draws off the low-boiling medium from the tank to the regenerator, where part of the heat from the medium is recovered after its discharge from the turbine. The medium is then directed into the evaporator, from which, in the form of vapor, it flows towards the turbine blades. Subsequently, the working medium flows into the regenerator and into the condenser, from where it is delivered to the tank, and so the cycle continues.

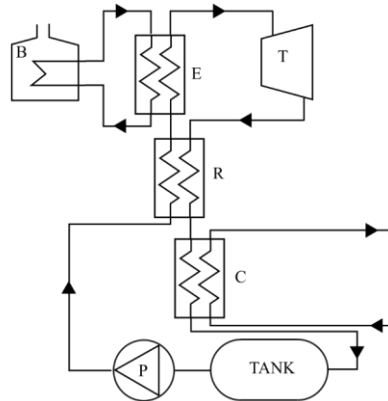


Fig. 1. Diagram of the ORC system  
(T – turbine, B – boiler, E – evaporator, R – regenerator, C – condenser, P – pump)

It is estimated that the low-temperature waste heat represents more than 50% of the total heat generated by industry [3]. ORC installation enables heat recovery from low-temperature sources (e.g. industrial waste heat, biomass combustion, geothermal heat, etc.). In such installations, a low-temperature heat is converted into useful work, that can itself be converted into electricity. This process is not feasible with conventional working mediums [4]. In order to recover low-grade heat by means of an ORC system, the working medium must have a lower boiling temperature than water. Both radial-flow [5] and axial-flow turbines [6] as well as expanders [7] are applied in ORC systems. CES 36 working fluid was used in the axial-flow turbine [8].

Energetic turbines are such devices for which operational reliability and efficiency are of key importance [9,10]. It is absolutely necessary to ensure durable components [11]. Equally important here is to regularly check the operating temperature, which was highlighted in the paper [12]. Energetic turbines' dynamic properties, as described in the article [10], are strongly influenced by residual unbalance [13] and axial forces acting on the turbine stage(s).

## 2. MODEL DESCRIPTION

The nominal speed of the designed five-stage turbine is 3000 rpm. The turbine shaft was made of 40 HM constructional steel and it weighs about 240 kg. Fig. 2 shows the turbine rotor model created by means of FEM (Finite Element Method). The radial bearings mounting points are indicated by the two arrows.

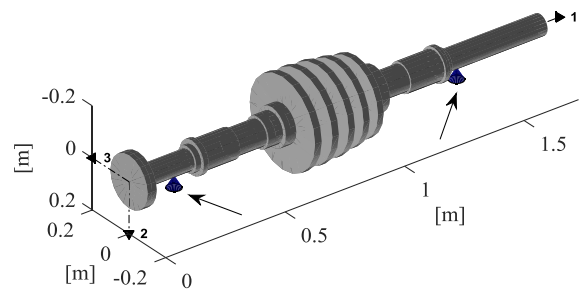


Fig. 2. 3D model of the turbine rotor

The numerical analyses were carried out using MADYN 2000 (commercial software) and KINWIR-I, NLDW in-house developed computer programs included in the MESWIR system. This system was developed at the IFFM PAS in Gdańsk. The model created in Madyn 2000 is presented in Fig. 3, it comprised 52 beam elements.

The shaft length was 1.646 m. The distance between the two journal bearings was 1.164 m, they were located in the nodes numbered as 10 and 46. The thrust bearing and torsional vibration damper were positioned at the nodes no. 7 and no. 51, respectively. The thrust bearing was modeled using the following parameters: stiffness in the axial direction  $1.5 \cdot 10^9$  N/m and damping  $8.5 \cdot 10^6$  Ns/m. The value of  $1.0 \cdot 10^9$  Nm/rad was adopted as stiffness of the torsional vibration damper. Five stages of the turbine were modeled as turbine rotor disks which were located in the nodes numbered as 27, 29, 31, 33 and 35. The residual unbalance of 2500 gmm ( $0.025 \text{ kg} \times 0.1 \text{ m}$ ) was placed in the node no. 29. This value was selected in accordance with standard ISO 1940-1 [14]. The mechanical seals were at the nodes: 19, 22 and 38.

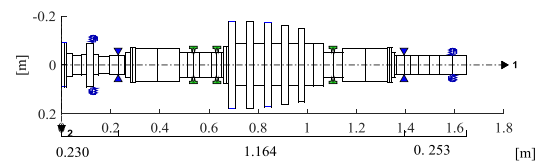


Fig. 3. FEM model of the rotor based on a modeling by beam elements

## 3. KINETOSTATIC ANALYSIS

Two load cases were taken into consideration, leading to two separate computations. In the first case, the load resulted directly from the action of gravitational force. In the second case, the rotor disk forces (caused by flow of the working medium) were taken into account during computations. Tab. 1 summarizes the loads affecting the turbine rotor disks.

Tab. 1. Forces and bending moments of the turbine rotor disks

| no. | force [N] | bending moment [Nm] |
|-----|-----------|---------------------|
| 1   | 11245     | 448.5               |
| 2   | 5535      | 449.5               |
| 3   | 4281      | 443.7               |
| 4   | 4350      | 435.8               |
| 5   | -2072     | 421.8               |

Fig. 4 presents the shearing forces and bending moments acting on the turbine rotor and the response of bearing supports obtained for the first load case. These values were higher than the values obtained in the second computation. The reactions at radial bearings supports were approximately 1200 N. The maximum value of the bending moment was observed within the middle part of the shaft and was around 400 Nm. After performing kinetostatic computations for the second load case (taking into account axial forces), it turned out that the reaction of the hydrodynamic axial bearing was 23 300 N.

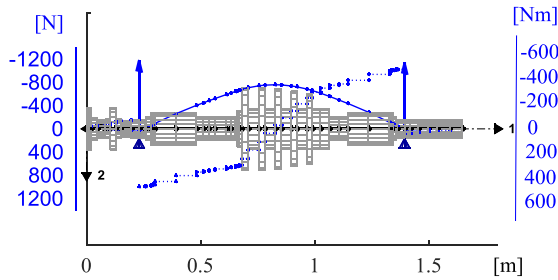


Fig. 4. Rotor static load. The shearing forces and bending moments are marked with dashed lines and continuous lines, respectively. The vectors represent static reactions of the rotor supports

The graph of shaft displacements for the first computation variant was shown in Fig. 5. The maximum displacement was around 30 μm (in the central part of the shaft).

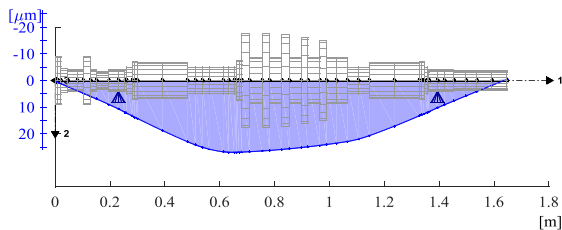


Fig. 5. Shaft displacements obtained for the first computation variant

Fig. 6 presents the reduced stress of the turbine shaft resulting from external forces. These values do not exceed the value of 50 MPa, which is more than four times lower than the admissible value.

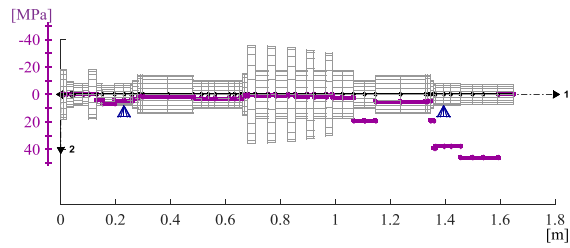


Fig. 6. Values of the shaft's reduced stress obtained for the second computation variant

#### 4. MODAL ANALYSIS

The modal analysis was carried out in the frequency range from 0 Hz to 500 Hz. The first nine mode shapes were analyzed. The first mode shape, which was classified as lateral mode was presented in Fig. 7. It represents a cone-shaped vibration at 28 Hz. The second lateral mode shape manifests itself in the form of a cylinder-shaped vibration at 30 Hz, as shown in Fig. 8.

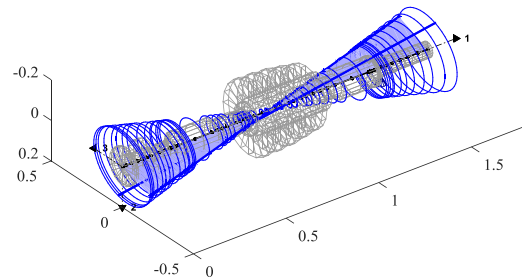


Fig. 7. The first lateral mode shape of the rotor – cone-shaped vibration at 28 Hz

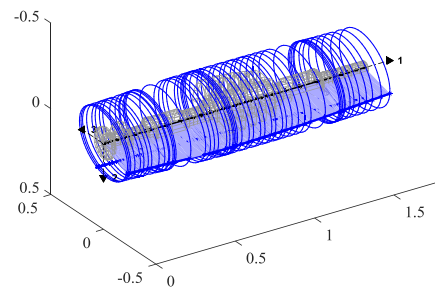


Fig. 8. The second lateral mode shape of the rotor – cylinder-shaped vibration at 30 Hz

A very important mode shape is the first bending mode shape, from the point of view of dynamic stability. This mode shape was presented in Fig. 9. If the eigenfrequency of a first bending mode shape coincides with the frequency that corresponds to nominal operating speed (or its multiples) the vibration of a very large amplitude may occur. In the case at hand, the first transverse mode shape manifests itself at a frequency of 124 Hz.

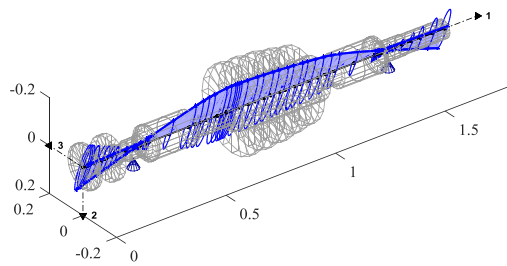


Fig. 9. The first bending mode shape of the rotor at 124 Hz

Following a modal analysis, the original construction has been substantially redesigned. The first variant of the rotor geometry was optimized since the natural frequency corresponding to the first bending mode shape of the rotor coincided with the frequency corresponding to the nominal operating speed. After this modification the first transverse mode shape manifested itself at 124 Hz and hence within the safe range.

## 5. GEOMETRY OPTIMIZATION FOR BEARINGS

In order to ensure proper operating conditions for a fluid-flow machine, the careful selection of bearings along with their geometry is strongly recommended. That is why the bearings of various widths and of varying clearance sizes were analyzed by the authors of this paper. As a result of this analysis the journal diameter value of 80 mm was selected for the radial bearings.

Fig. 10 and Fig. 11 illustrate the journal displacements obtained for the bearing with a width/diameter ( $L/D$ ) ratio of 0.5. The computations were carried out across a wide range of rotational speeds, i.e. from 1 500 rpm to 9 000 rpm. The parameters such as bearing clearance size and bearing width must have been so selected as to minimize vibration level at the nominal speed (3000 rpm). It was also important to keep the resonant vibration amplitude (that occurred at the rotational speed of around 7000-7500 rpm) as low as possible.

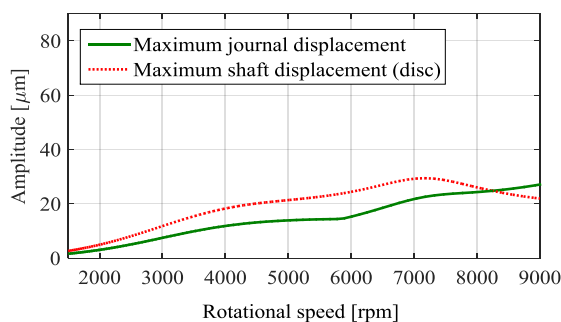


Fig. 10. Vibration amplitudes of the bearing with the following basic design parameters:  $L/D = 0.5$ ,  $\Delta R = 40 \mu\text{m}$

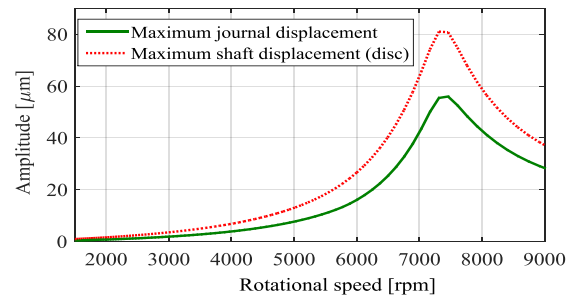


Fig. 11. Vibration amplitudes of the bearing with the following basic design parameters:  $L/D = 0.5$ ,  $\Delta R = 80 \mu\text{m}$

During the analysis, the bearing width ( $L$ ) was adjusted, and consequently, the width/diameter ratio as well as size of the bearing clearance ( $\Delta R$ ). Minor changes in geometry of the bearings had a major impact on the vibration amplitude. The values of maximum journal displacements for the bearing located at the node no. 10 are shown in Fig. 12.

As the bearing width increases, the vibration amplitude at nominal speed decreases. Furthermore, as the bearing clearance decreases, the vibration amplitude at nominal speed decreases, while that at resonant speed (approx. 7 000 rpm) increases.

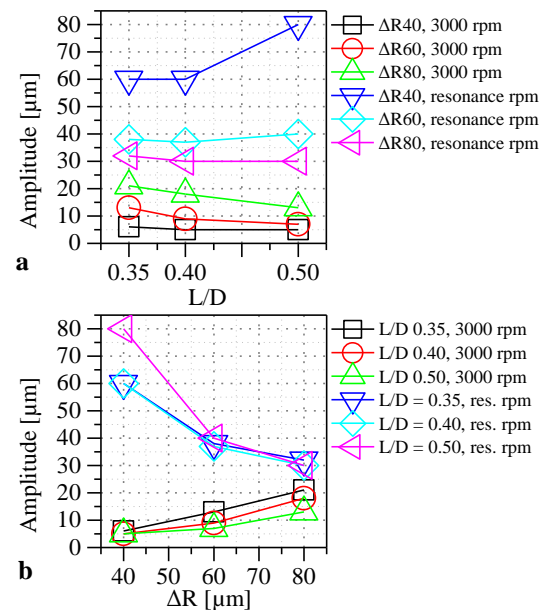


Fig. 12. **a** Journal displacement as a function of  $L/D$  ratio. **b** Journal displacement as a function of bearing clearance ( $\Delta R$ )

On the basis of the analysis presented, the bearing with the width of 40 mm ( $L/D = 0.5$ ) and radial clearance of  $60 \mu\text{m}$  has been chosen.

## 6. LEMON BORE JOURNAL BEARINGS

Change in shape of the bearing clearance was also analyzed. Apart from the most common bore profile (bearing with a cylindrical bore), also a lemon bore bearing was examined. In this respect,

the computations were carried out using computer programs included in the MESWIR series. Geometric differences between two bore profiles used in journal bearings are shown in Fig. 13.

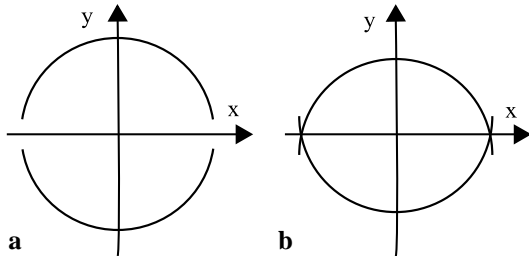


Fig. 13. Two bore profiles used in journal bearings: **a** cylindrical bore, **b** lemon bore

During simulation studies the following assumptions have been made: in the cylindrical bore bearings radial clearance was 60 μm, in the lemon bore bearings the horizontal clearance was 60 μm and vertical clearance was 40 μm.

In both cases, the bearings had the diameter of 80 mm and the width of 40 mm.

Two pockets with an arc of 20° were modeled. The lubricating oil had the following parameters: dynamic viscosity — 0.017 Ns/m and supply pressure — 5·10<sup>4</sup> N/m<sup>2</sup>.

The computations were performed in the rotational speed range 1 400 ÷ 9 000 rpm. Fig. 14 presents the vibration amplitude curves as a function of rotational speed for both bearing types. The vibration amplitudes of the node no. 29 (second disk) are shown as broken lines, while that of the node no. 7 (bearing journal) are shown as continuous lines.

The computation results demonstrate that the application of lemon bore bearings has reduced the maximum vibration amplitude of the journal by 1.5 μm (from 7.5 μm to 6 μm) at the nominal speed (3000 rpm), while that amplitude has increased from 47.5 μm to 100 μm at the resonant speed (7000 rpm).

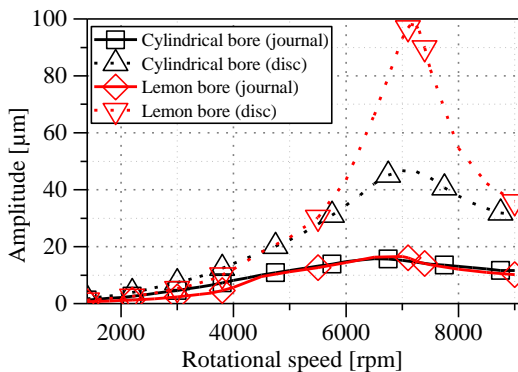


Fig. 14. Amplitude - speed characteristic for cylindrical/lemon bore bearings

Depending on the shape of the bearing clearance the altered shape of vibration trajectories was

observed. The exemplary bearing journal trajectories for the resonant speed (approx. 6 500 rpm) are presented in Fig. 15.

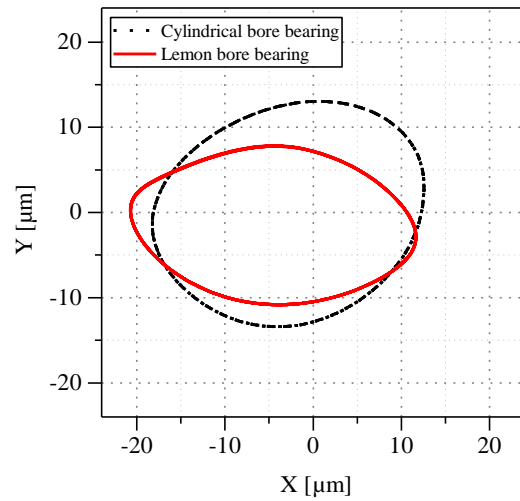


Fig. 15. The trajectories of journal vibrations for the cylindrical bore and lemon bore bearing at the rotational speed of 6 500 rpm

## 7. ANALYSIS OF THE THRUST BEARINGS

The kinetostatic and dynamic analyses of the dynamical system have been preceded by computations of bearing coefficients carried out in the MESWIR system. Thrust bearing characteristic was determined for a specified value of total external load. The values of the following parameters were identified: minimum size of bearing clearance, segment's angle of incline, pressure distribution, segment's and bearing's stiffness and damping.

The basic parameters of the axial bearing were as follows: internal diameter  $D_i = 0.098$  m, segment's width  $B = 0.061$ , number of segments  $N = 6$  and total external load  $Q_e = 23300$  N.

The computed values for the bearing stiffness was  $-1.52351 \cdot 10^9$  N/m and for the bearing damping was  $-8.46763E \cdot 10^6$  Ns/m. Fig. 16 demonstrates one segment and the pressure distribution on the surface. Maximum pressure was 1.8721 MPa.

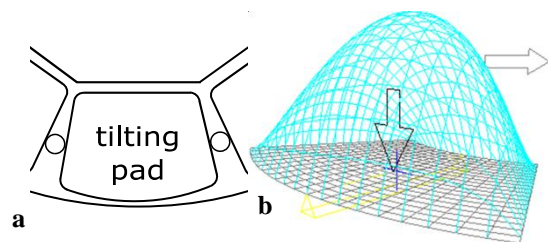


Fig. 16. **a** Schematic view of one segment of the thrust bearing. **b** Pressure distribution within the segment of the thrust bearing

## 8. SUMMARY AND CONCLUSIONS

In this article the process of numerical calculation of the newly developed ORC turbine has been described. The energetic turbine's design process requires a multistage analysis and usage of modern tools. In order to ensure proper dynamic properties, an optimization of rotor geometry and selection of appropriate bearings is needed.

Madyn 2000 software was used to carry out kinetostatic, dynamic and modal analyses of the rotor supported by cylindrical bore hydrodynamic bearings. Moreover, the dynamic computations related to various bore profiles (cylindrical/lemon bore) and the multi-segment thrust bearing were conducted by means of the in-house developed computer programs included in the MESWIR system, created at the IFFM PAS.

After performing a modal analysis it turned out that the rotor with the flow-optimized shape should be substantially redesigned. The first bending mode shape was dangerously close (5 %) to nominal rotational speed (3 000 rpm). After the modification of the geometry it occurred at 124 Hz.

The kinetostatic analysis has shown that the displacement values are low and the shaft's reduced stress is within the limits of the relevant standards.

The analysis performed was based on changes in bearing clearance and width. The maximum vibration amplitude was analyzed in two shaft locations (at the disk and at the bearing journal) for various bearing configurations. The authors of the article made the following observations:

- vibration amplitude decreases as bearing's width increases (at the nominal rotational speed),
- vibration amplitude decreases at the nominal speed and increases at the resonant speed, together with a clearance decrease.

The analysis of hydrodynamic radial bearings with two various bore profiles (cylindrical/lemon bore) has been carried out. The application of a lemon bore profile in the bearing caused the following changes in the vibration amplitude: the amplitude decreased slightly at the nominal speed and increased slightly at the resonant speed. Cylindrical bore bearings were chosen for further analysis because they are easier to manufacture than lemon bore bearings. Despite of the fact that the article is a case study, the results could be applicable to turbines belonging to this class of machines.

Apart from the radial bearings, the axial bearings were also analyzed. All analyses presented in this article confirmed good dynamical properties of a newly designed turbine operating in an ORC installation. The results of these studies have significantly contributed to the geometry of the ORC turbine, which is to be used at the steelworks in China.

## REFERENCES

1. Li Y, Ren XD. Investigation of the organic Rankine cycle (ORC) system and the radial-inflow turbine design. *Applied Thermal Engineering*. Elsevier Ltd; 2016;96:547–54.
2. Cao Y, Gao Y, Zheng Y, Dai Y. Optimum design and thermodynamic analysis of a gas turbine and ORC combined cycle with recuperators. *Energy Conversion and Management*. Elsevier Ltd; 2016;116:32–41.
3. Hung TC, Shai TY, Wang SK. A review of organic rankine cycles (ORCs) for the recovery of low-grade waste heat. *Energy*. 1997;22(7):661–7.
4. Kiciński J, Żywica G. *Steam Microturbines in Distributed Cogeneration*. Springer monograph; 2014.
5. Kang SH. Design and experimental study of ORC (organic Rankine cycle) and radial turbine using R245fa working fluid. *Energy*. Elsevier Ltd; 2012;41(1):514–24.
6. Hun S. Design and preliminary tests of ORC (organic Rankine cycle) with two-stage radial turbine. *Energy*. Elsevier Ltd; 2016;96:142–54.
7. Kaczmarczyk TZ, Ihnatowicz E. The experimental investigation of scroll expanders operating in the ORC system with HFE7100 as a working medium. *Applied Mechanics and Materials*. 2016;831:245–55.
8. Desideri A, Gusev S, Broek M Van Den, Lemort V, Quoilin S. Experimental comparison of organic fluids for low temperature ORC systems for waste heat recovery applications. *Energy*. Elsevier Ltd; 2015;97:460–9.
9. Dynamics T, Gen D. Experimental Investigation of a Radial Microturbine in Organic Rankine Cycle system with HFE7100 as working fluid. *Proceedings of the 3rd International Seminar on ORC Power Systems*. 2015;1–10.
10. Kaczmarczyk TZ, Żywica G, Ihnatowicz E. The experimental investigation of the biomass-fired ORC system with a radial microturbine. *Applied Mechanics and Materials*. 2016;831:235–44.
11. Żywica G, Drewczyński M, Kiciński J, Rządkowski R. Computational modal and strength analysis of the steam microturbine with fluid-film bearings. *Journal of Vibrational Engineering and Technologies*. 2014;2(6):543–9.
12. Kaczmarczyk TZ, Żywica G, Ihnatowicz E. Thermographic investigation of the cogenerative ORC system with low-boiling medium. *Diagnostyka*. 2015;16(3):25–32.
13. Żywica G, Kiciński J. The influence of selected design and operating parameters on the dynamics of the steam micro-turbine. *Open Engineering*. 2015;5(1):385–98.
14. ISO 1940-1 Mechanical vibration - balance quality requirements for rotors in a constant (rigid) state. Part 1: Specification and verification of balance tolerances.

Received 2016-03-24

Accepted 2016-04-13

Available online 2016-06-04



**Lukasz BREŃKACZ**, received MSc Eng. degree in Mechanical Engineering in 2011 and Eng. degree in Informatics in 2013 from the University of Warmia and Mazury, Olsztyn, Poland. Currently he works at the Institute of Fluid-Flow Machinery Polish Academy of Sciences, Gdańsk, Poland as a research assistant. He is a PhD student at Gdańsk

University of Technology, Gdańsk, Poland. His current research interests include designing, computer simulation and experimental diagnostics of rotating machinery.



**Grzegorz ŻYWICA**, PhD, Eng. Since 2005 has been working at the Institute of Fluid-Flow Machinery PAS in Gdańsk. Since 2014 he is the head of the Department of Turbine Dynamics and Diagnostics. His scientific work focuses primarily on computational simulation, designing of rotating machinery and bearing systems, modal

analysis and technical diagnostics.



**Malgorzata BOGULICZ**, MSc. is a specialist in the Department of Turbine Dynamics and Diagnostics PAS in Gdańsk. Her main research areas are: numerical calculations, development of computer application